

See discussions, stats, and author profiles for this publication at: <https://www.researchgate.net/publication/324589867>

Soil–geomorphology relationships and landscape evolution in a southwestern Atlantic tidal salt marsh in Patagonia, Argentina

Article in *Journal of South American Earth Sciences* · April 2018

DOI: 10.1016/j.jsames.2018.04.015

CITATIONS

3

READS

186

4 authors:



Ileana Ríos

Instituto Patagónico para el Estudio de los Ecosistemas Continentales (IPEEC-CO...

6 PUBLICATIONS 44 CITATIONS

[SEE PROFILE](#)



Pablo Bouza

Centro Nacional Patagonico

56 PUBLICATIONS 560 CITATIONS

[SEE PROFILE](#)



Alejandro Bortolus

Centro Nacional Patagonico

72 PUBLICATIONS 1,895 CITATIONS

[SEE PROFILE](#)



María del Pilar Álvarez

National Scientific and Technical Research Council

21 PUBLICATIONS 83 CITATIONS

[SEE PROFILE](#)

Some of the authors of this publication are also working on these related projects:



Eco-Taxo Interfase [View project](#)



Late Cenozoic of Peninsula Valdés, Patagonia, Argentina. [View project](#)



Soil-geomorphology relationships and landscape evolution in a southwestern Atlantic tidal salt marsh in Patagonia, Argentina

Ileana Ríos*, Pablo José Bouza, Alejandro Bortolus, María del Pilar Alvarez

Instituto Patagónico para el Estudio de los Ecosistemas Continentales (IPEEC-CONICET), Boulevard Brown 2825, CP U9120 ACF, Puerto Madryn, Chubut, Argentina



ARTICLE INFO

Keywords:

Hydromorphic soils
Grain-size distribution
Semi-desert salt marsh
Carbon stable isotopes
Vascular plants

ABSTRACT

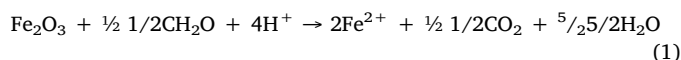
Salt marshes in Patagonia ecosystem are nowadays fully recognized by ecological, pollution and phytoremediation studies but a soil genesis and geomorphology approach is currently unknown. The aim of this study was to establish the soil-geomorphology relationship in Fracasso salt marsh and to determine the successional vegetation dynamics associated with the landscape evolution. This work was carried out in Fracasso salt marsh sited in Península Valdés, Argentina, where an integrated study on soil-geomorphology relationship and landscape evolution was performed along with sedimentological analysis and vegetation changes (C3 photosynthesis pathway vs. C4 photosynthesis pathway plants). This last was determined through the $\delta^{13}\text{C}$ composition from soil organic matter (SOM). Soil descriptions and laboratory analysis of soil samples were performed. A marked relationship between the vegetation unit, the dominant landform and the type of associated soil was found. *Limonium brasiliense* (Lb) and *Sarcocornia perennis* (Sp), both C3 plants, are dominant in levees associated with tidal creeks, and soils were classified as Typic Fluvaquents, while *Spartina alterniflora* (Sa) soils were classified as Sodic Endoaquents and Sodic Psammaquents. Although no sulfidic materials were identified by incubation test, they were identified by hydrogen peroxide treatment in Sa soils, and now are considered potential acid sulfate soils (PASS). Sedimentological analysis from deepest sandy C horizons indicates a beach depositional environment. On the other hand, the $\delta^{13}\text{C}$ stable isotope composition of SOM preserved into these buried soil acting as parent materials shows the dominance of C4 plants presumably belonging to *Spartina* species, suggesting a possible colonization and stabilization as the pioneer salt marsh.

1. Introduction

Tidal salt marshes are peculiar environments placed in the highest part of the intertidal zone where a muddy substrate generally supports a wide range of halophyte vegetation (Allen and Pye, 1992). These environments are formed according to the variations of sea level occurred during the Holocene and they are frequently flooded and subjected, not only to marine action, but also to the influence of water and continental sediments, either from estuary system or from surface runoff. This is why salt marsh soils have a very weak profile development, most of them belonging to Entisols Order and Aquents Suborder in places where aquic moisture regime prevails (Soil Survey Staff, 2014).

Anoxia and salinity conditions would be both sufficient to produce sulfidic materials (potential acid sulfate soils; Soil Survey Staff, 1999) due to the buildup and stability of sulphides, mainly pyrite, which comes from the biological reduction of sulphate dissolved in seawater and Fe^{3+} from marine sediments. This Fe^{3+} and SO_4^{2-} reduction is responsible for pH increase (Van Breemen, 1993; Konsten et al., 1994,

Eqs. (1) and (2)). Therefore, sulfidic materials soils are classified as Sulfaquents (Great Group level, Soil Survey Staff, 1999).



Salt marsh soils are closely related with landforms, sedimentation processes and vegetation (Redfield, 1972; Fagherazzi et al., 2004). A first complete description of the main salt marsh landforms was made by Benito and Onaindia (1991) on the Mundaka-Urdaibai salt marsh (Basque Country, Northeastern Spain). They considered tidal channels as one the most important salt marsh landforms because of the exchange of matter and energy between the salt marsh and the ocean (Mitsch and Gosselink, 2000). In this way, linear channels are typical of the first stages of salt marsh evolution and, over the time, they evolve to more complex forms such as dendritic or meandric-dendritic forms (Pye and French, 1993). Levees are another important salt marsh landform formed in the edge of the tidal channels as a consequence of

* Corresponding author.

E-mail address: irios@cenpat-conicet.gov.ar (I. Ríos).

sea water flow. In this way, during the flooding, a rapid sand sedimentation occur showing a pattern of grain size decreasing with the distance from the channel to the inner marsh (Friedrichs and Perry, 2001). As regards vegetation, Zedler et al. (1999) established a relationship between this variable and marsh elevation in California salt marshes. Therefore, Otero and Macias (2001) related the physiographic position with the dominant vegetation in order to characterize the main salt marsh soils.

Particularly, botanical zonation is the most common salt marsh characteristic worldwide which can be observed in a generalized cross-section of the salt marsh coastline, where soil conditions such as salinity, saturation, immersion and anoxia are highlighted by a pattern roughly parallel to the coast (Pennings and Callaway, 1992; Silvestri et al., 2005). This pattern could reflect ecological succession assuming that bare soils of the tidal flats are colonized by typical low marsh species that promote soil accretion by trapping sediment and producing land elevation. This would enable the colonization of other species and eventually, the first colonizing plants would disappear, possibly settling in the lower levels of the marsh (Leeuw et al., 1993; Steers, 1977). However, changes in vegetation may also be due to changes in sea level, continental water and sediment discharges or any other possible event (e.g. storminess) or geomorphological and sedimentological processes (e.g. changes on depositional regimes and sediment autocompaction) which took place during Holocene (Allen et al., 2006; Choi et al., 2001; Goman et al., 2008; Lamb et al., 2006, 2007).

One way to determine past changes in the vegetation and the geomorphology is by assessing the proportion of plants C4/C3 through $\delta^{13}\text{C}$ isotopic compositions from soil organic matter (SOM) which is recorded in the soil profile (Chmura and Aharon, 1995; Choi et al., 2001; Lamb et al., 2006, 2007). This is based on the discrimination of plants with respect to CO_2 during the process of photosynthesis, which is due to the biochemical properties of primary enzymes that fix carbon and to the diffusion process that controls the CO_2 entry in leaves (Farquhar et al., 1989). This type of discrimination varies according to the photosynthetic cycles C3, C4 and CAM of the terrestrial plants. C3 plants reduce CO_2 to phosphoglycerate (3C) via the ribose biphosphate/oxygenase enzyme (Rubisco). That is why the plants with this type of photosynthesis have a $\delta^{13}\text{C}$ of -32‰ to -22‰ with an average of -27‰ (Boutton, 1991). They are best adapted to cool and wet environments. Unlike C3 plants, C4 plants reduce CO_2 to aspartic or malic acid (4C) via the enzyme phosphoenolpyruvate carboxylase (PEP). These plants discriminate less ^{13}C so they have higher values in $\delta^{13}\text{C}$ than the C3 plants. The isotopic range for this plant type is -17‰ to -9‰ with an average of -13‰ . (Boutton, 1991). They are best adapted to hot, sunny environments which implies an evolutionary advantage on C3 plants regarding to global warming. For example, in a northern Patagonia salt marsh, in the low position, where waterlogging conditions prevail almost permanently, *Spartina alterniflora* (C4 pathway) species is dominant and tolerant to salt stress (Mendelsohn and Morris, 2002; Bortolus et al., 2015) and soil anoxia (Bertness, 1991; Idaszkin et al., 2011). Whereas in the high marsh position, where the water table is about tens centimeters deep, *Sarcocornia perennis* (C3 pathway) are dominant (Bortolus et al., 2009; Idaszkin et al., 2011).

In addition, in order to determine if the SOM is autochthonous (i.e. it contains terrestrial components such as lignin, cellulose and humic substances) or allochthonous (it contains marine components), the weight ratio of organic carbon to total nitrogen (C:N) is used. Lamb et al. (2006) established that C:N ratios higher than 12 suggest that organic matter is from terrestrial sources. On the contrary, the allochthonous component coming from aquatic organisms tends to balance at a C:N ratio ranging from 4 to 10, indicative of organic matter without cellulosic structures from algae and phytoplankton.

In view of the foregoing, research on salt marshes on Extra-Andean Patagonian coast has focused mainly on ecological, pollution and phytoremediation aspects (Bortolus et al., 2009; Idaszkin and Bortolus, 2011; Idaszkin et al., 2011, 2014, 2015, 2017). As regards the pedology

and geomorphology approach, Bouza et al. (2008) carried out a preliminary study describing salt marsh soils and classified the main Patagonian salt marshes. In addition, Playa Fracasso, a salt marsh of great ecological interest (Bala et al., 2008; Idaszkin et al., 2011), has only been focused from multi-disciplinary studies such as soil-plant relationship, hydrological-geomorphological relationship, and salinization processes (Ríos, 2015; Alvarez et al., 2015, 2016). Moreover, integrated studies on soil – geomorphology relationship and geo-ecology are scarce, mainly those aimed at elucidating landscape evolution, ecological processes (e.g. ecological succession) and geochemical processes. Considering all the above mentioned, the aim of this study was to establish the soil-geomorphology relationship in Playa Fracasso salt marsh and to determine the successional vegetation dynamics associated with the landscape evolution. The results will substantially increase the knowledge about salt marsh soils and eco-geomorphology, and will be useful to apply successful conservancy strategies for these environments in the protected area of Península Valdés.

1.1. Study area

Península Valdés (PV) is a 3600 km² area located on the Patagonia east coast between parallels 42°05' and 42°53'S and meridians 63°05' and 64°37'W connected to the mainland by the Istmo Carlos Ameghino (Carlos Ameghino Isthmus) which is only 11 km wide and less than 30 km long (Fig. 1). That is the reason why PV is almost an island that belongs to the Patagonian steppe, a cool semi-desert environment which surrounds it. It has a dynamic coastal zone with active sand dunes, numerous cliffs, spits, bays and coastal lagoons. The inside land is a desert steppe with dry climate and strong winds. UNESCO designated PV as a World Heritage Site list in 1999 because its coast and gulfs have global significance for the conservation of marine mammals (e.g. southern right whale). And following the ecological approach, PV is considered a transition area between two phytogeographic provinces (Monte and Patagonia) and two marine biogeographic regions (Argentina and Magallanica) which results in the richest diversity of marshes with both, muddy and rocky bottoms. In particular, the *Spartina*-dominated muddy bottom marshes are found in PV northern area ($\leq 42^\circ\text{S}$) and the *Sarcocornia*-dominated muddy marshes in the south ($> 42^\circ\text{S}$) (Bortolus et al., 2009).

The study area corresponds to the so-called Playa Fracasso (PF) salt marsh, northeast of the Istmo Carlos Ameghino (Fig. 1) on the Golfo San José (San José Gulf) margins. This gulf splits longitudinally into two hydrographic domains (east and west) by a climatic frontal system. The west circulation domain of the current is driven by well-defined vortices at the edge of the mouth whereas in the east domain -where the present study was performed-the conditions are more stagnant (Amoroso and Gagliardini, 2010). Fracasso salt marsh had a muddy plain built up by deposition of very fine grains produced by decantation and retention of halophyte plants. This salt marsh was protected by high sand bars, presumably due to both an exceptional storm and an extraordinary tide. The salt marsh was dominated by tides and exhibits a pattern of accretion. This pattern was largely controlled by the distribution of tidal channels and creeks and ephemeral alluvial sediment inputs from the mainland. The surrounding salt marsh geologic units are represented mainly by tertiary marine rocky sediments of Puerto Madryn Formations (Middle Miocene), and by the sandy-gravel deposits called “Rodados Patagónicos” (RP) of Plio-Pleistocene age (Haller, 1981; Haller et al., 2001). These Neogene-Quaternary units outcrop both on active cliffs and on erosion scarps of the littoral piedmont. The Holocene, which partially covered these geological units, is formed by colluvial, alluvial, aeolic, and coastal marine deposits. In the study area the average annual precipitation is 246 mm and the average annual temperature is 12.5 °C. The tidal regime is semi-diurnal with an average value of amplitude between 7.01 and 4.57 m.a.s.l. (SHN, Servicio de Hidrografía Naval Argentino, 1983). Considering that Playa Fracasso in PV has been identified as one of the

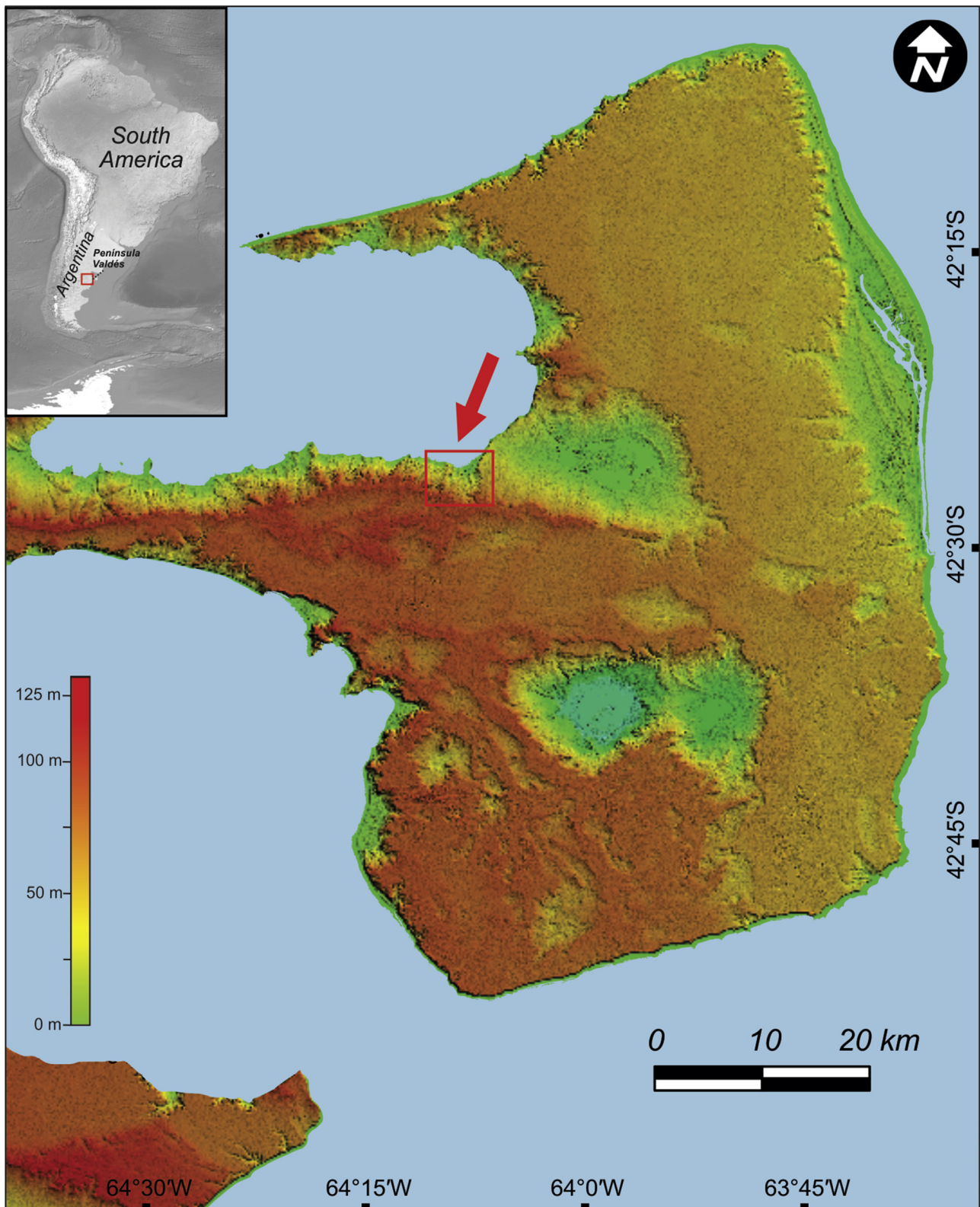


Fig. 1. Location of the study site, Fracasso salt marsh, Península Valdés.

main wetlands of the Patagonian coast, it has been declared one of the Wetlands of International Importance by the RAMSAR Convention on Wetlands and has been included in the Hemispheric Reserve Network for Shorebirds.

2. Materials and methods

2.1. Field work

To determine the relationship between landforms, soils and vegetation, three communities of the most dominant vegetation –S.

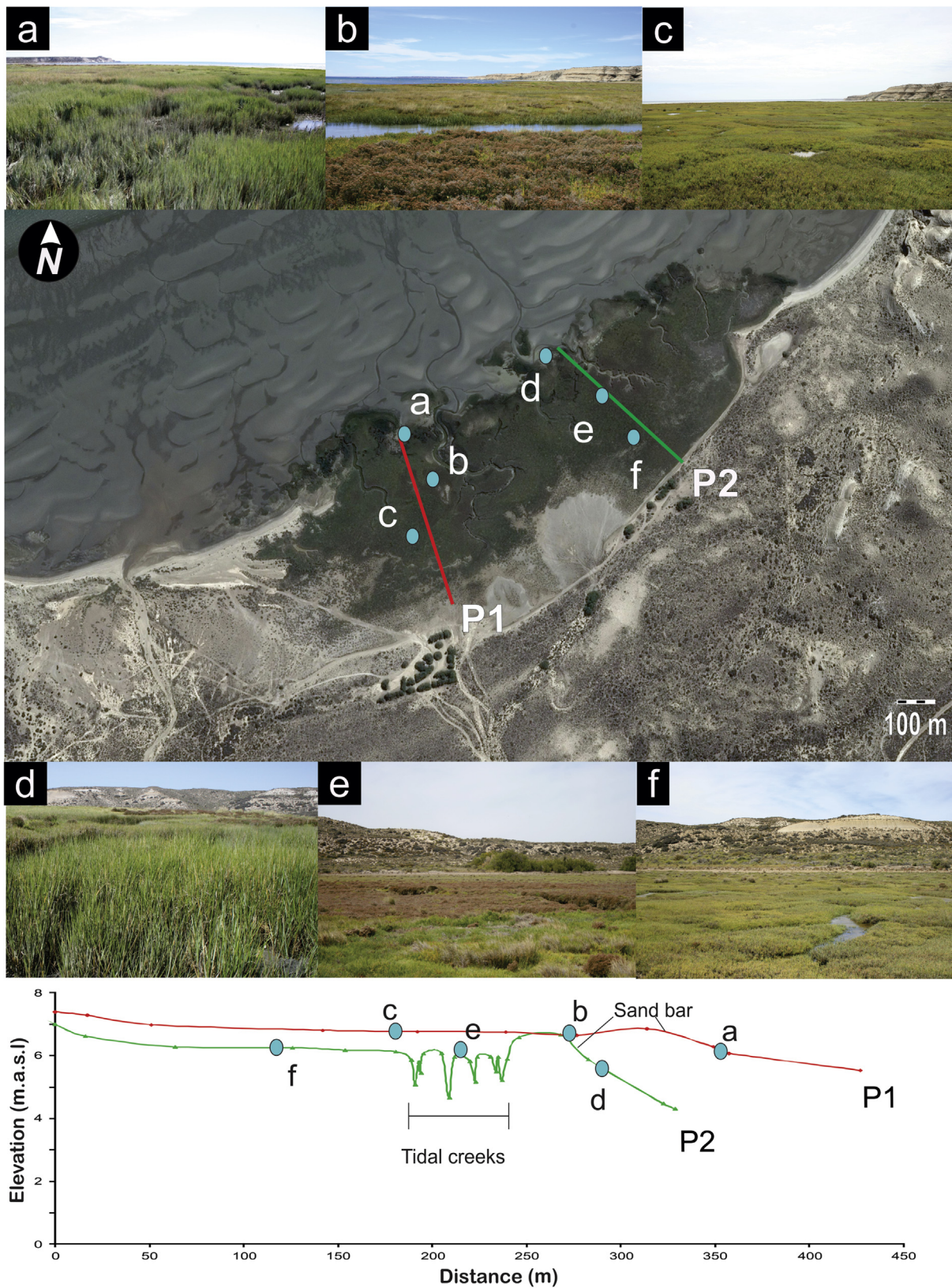


Fig. 2. View of the main vegetation unit's landscape and geomorphology. Sand inter bar (Sa1, a) and sand bar (Sa2, b) in *S. alterniflora*, levees zones in *L. brasiliense* (Lb1, Lb2, c and d) and flooding planes in *S. perennis* (Sp1, Sp2, e and f). On the bottom the exactly topographic position of each vegetation unit is shown.

alterniflora (Sa), *L. brasiliense* (Lb) and *S. perennis* (Sp) – were described and associated with landform elements (Fig. 2). The term *landform element* is used in this study to define different geomorphic processes observed in the salt marsh (e.g. shallow pans, sand bars, dunes, alluvial

fans, tidal creek, levees of the tidal creeks, point bars of the tidal creeks, mud flats). The landform elements (with relatively homogeneous vegetation patterns) were delimited by aerial photographs (1:20,000; SHN) and Google Earth® satellite images. Two topographic transects (P1

and P2, Fig. 2) perpendiculars to the shoreline were performed by an optical level Kern GK1-AC in order to identify the plant zonation and soil landform distribution. The 0-level was estimated considering an annual maximum extraordinary low tide according to the tide table provided by the National Hydrographic Service (Fig. 2). A soil pit was made in the most representative area for each mappable landform element traversed by topographic transects. The designation of soil horizons, morphological description and soil sampling was performed according to Schoeneberger et al. (2012). Soil classification was made according to Soil Survey Staff (2014). Initial pH and Eh of each soil horizon was determined according to Faulkner et al. (1989) using an electrode of a portable digital pH/Eh-meter. The soil samples were zip-locked, taken to the laboratory and stored in hermetic containers at -4°C . A monitoring network was performed where the groundwater wells (piezometers) were positioned over the topographic transects and near the soil pits in order to analyze the groundwater ionic composition and to study the geochemical reactions that take place at the saturated zone. The wells were drilled with a hand auger up to a depth of 3 m and cased with 2.5-inch PVC tubes sealed at the bottom. A gravel filter was placed between the borehole and the casing, facing the permeable section, and then a layer of bentonite was added over the gravel pack to avoid a preferential vertical flow around the piezometer. Water samples were taken with bailers and water sample collection, preservation, and chemical analysis of major ions were carried out in accordance with the standard methods proposed by the American Public Health Association (APHA, AWWA and WPCF, 1997).

2.2. Laboratory processes and analytical determinations

At the laboratory, the soil samples were separated in two fractions: one was stored in freezer to -20°C and another was used to perform the analytical determinations. This last, was air-dried and sieved (2 mm mesh size) in order to separate the gravel and estimate its percentage. On the fine earth fraction ($< 2\text{ mm}$) the particle-size distribution was determined by the hydrometer method (Bouyoucos, 1962) after removal of organic matter with H_2O_2 30%. On sandy C horizons, the grain-size distribution of sand fractions was analyzed to determine the environment of deposition and to elucidate the marsh evolution (accretion process); that is, whether the buried sandy and loamy sand soil horizons corresponded to beach or coastal dune deposits. For this purpose, the actual sandy soil horizons (foreshore deposit, e.g. sand bars and tidal channel levee deposits) were analyzed. A typical characteristic of both beach and coastal dune deposits is the clean sand sediments, without pelitic fraction or suspension population (Visher, 1969; Andrews and Van der Lingen, 1969; Mazzoni, 1978). For this reason, the finest particles such as clay and silt were eliminated taking into account those fractions which more closely reflected the soil parent material composition (i.e. immobile fraction; Langohr et al., 1976). These finest particles (mobile fraction) could be present due to translocation from soil solution or to entrapping by pioneer vascular plants. The size particle analysis of sand fractions was performed using the Udden-Wentworth scale within the range 2000–62.5 microns at 0.5 phi (ϕ) intervals. To determine the depositional environments (e.g. beaches or dunes), the grain size distributions were plotted as cumulative frequency curves on arithmetic probability paper (Balsillie et al., 2002) and the Folk and Ward (1957) grain size parameters (mean grain size, sorting or standard deviation, skewness and kurtosis), were calculated by means of the Gradistat computer programme (Blott and Pye, 2001). Also, the comparative particle size distribution index (CPSDI; Langohr et al., 1976) was used to determine the degree of uniformity of the sandy soil parent materials. The CPSDI is the sum of the minimum values of the weight percentages of all granulometric fractions between two samples. It corresponds to the common area covered by two histograms made from granulometric data. A CPSDI of 100 indicates that between both horizons the particle size distribution is identical; a CPSDI of 0 indicates that the distribution curves do not overlap at all.

The CPSDI is derived as follows:

$$\text{CPSDI} = \sum_{i=1}^n mi$$

Where n is the number of fractions and mi is the lower weight percentage for each fraction i .

A CPSDI of 94–100 does cover the sampling and analytical errors. Consequently, an index of 94 or more attests for an extremely high similarity. Between 90 and 94 the index points samples are very similar and between 85 and 90 the similarity is high (Langohr and Van Vliet, 1979).

In order to characterize and classify the hydromorphic soils and their relationship to bearing capacity, the n -value was determined (Soil Survey Staff, 2014). For this index determination, the field capacity (FC) was estimated from soil texture according to Bodman and Mahmud (1932) procedure [FC (%) = 0.023 sand + 0.25 silt + 0.61 clay]. Soil samples were dried and screened through to 2 mm mesh size. For each subsample $< 2\text{ mm}$, soil pH was measured from 1:2.5 soil-water extract previously treated with hydrogen peroxide 30% (peroxide pH, pH_p; Ahern et al., 1998). A 1:2.5 soil-water extract was prepared from the fine earth and after 24 h the solution was vacuum pumped and its pH and electrical conductivity (EC) measured. The Ca^{2+} and Mg^{2+} contents in the soil solution were determined by EDTA titration, the Na^{+} and K^{+} by flame photometry, Cl^{-} by titration with silver nitrate, and SO_4^{2-} by the electroconductometric method. The water-soluble cation composition of the soil solution was used to calculate the exchangeable-sodium percentage (ESP) from sodium adsorption ratio (SAR; U.S. Salinity Laboratory Staff, 1954).

In order to determine the presence of sulfidic materials, incubation soil pH was measured once a week until stabilization, setting out soils under moist aerobic conditions (field capacity) at room temperature (initial pH, pH_i; incubation pH, pH_{inc}; Soil Survey Staff, 2014).

Cation-exchange capacity (CEC) was determined by saturating samples with 1 N Na-acetate at pH 8.2. Retained sodium in the exchange sites was extracted with 1 N NH_4^{+} -acetate at pH 7.0 and measured by flame photometry (Bower et al., 1952) after discarding the exchangeable cations. Total nitrogen was determined by micro-Kjedhal method and soil organic matter (SOM) was determined by ignition at 430°C (Davies, 1974) after dehydration at 105°C for 12 h. Soil organic carbon (C) was determined by dividing the organic matter content by the factor 1.72 (Page et al., 1982). Calcium carbonate equivalent was determined by gravimetric method (U.S. Salinity Laboratory Staff, 1954).

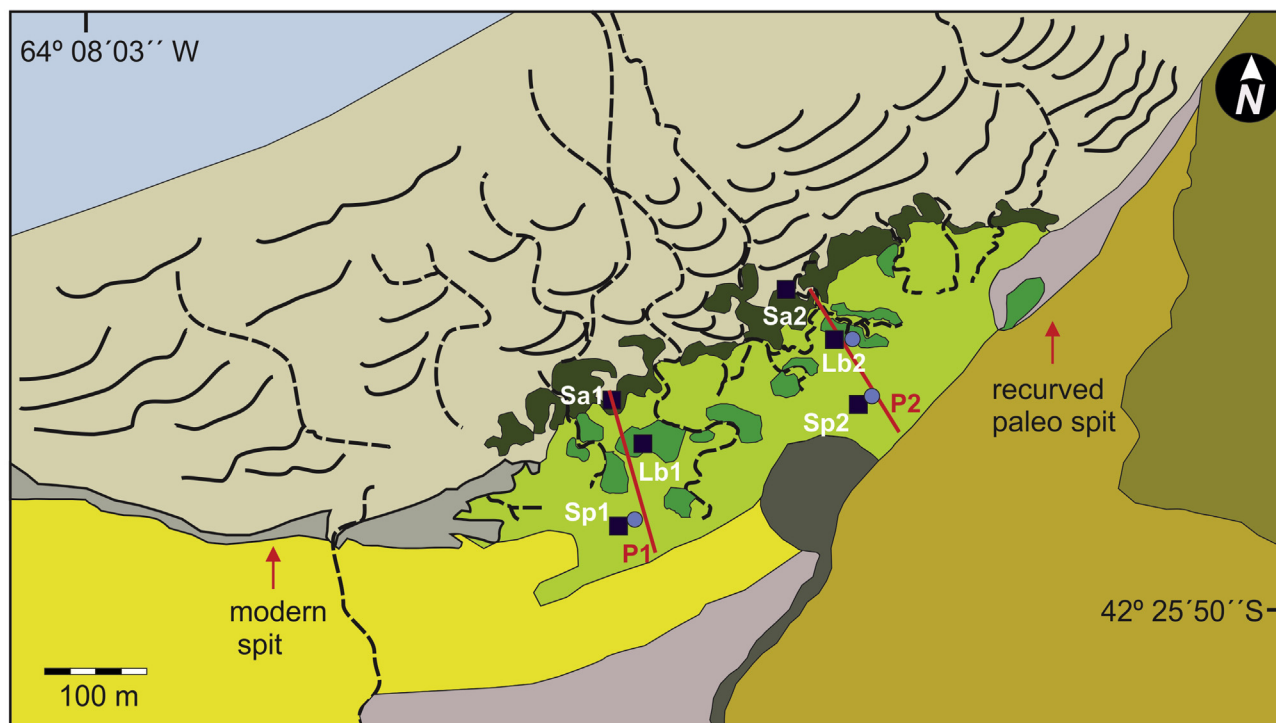
The isotopic compositions of $\delta^{13}\text{C}$ of soil organic carbon (bulk soil sample) and leaf plant tissues were determined by putting between 2000 and 8000 μg sample grounded at 0.5 mm sieve (40-mesh) and pretreating with HCl to remove inorganic carbon in tin capsules. Leaf plant tissues of *Spartina alterniflora*, *Sarcocornia perennis* and *Limonium brasiliense* were field harvested and laboratory cleaned in ultrasonic bath and oven-dried at 40°C . The grounded samples were analyzed in an elemental analyzer (Carlo Erba EA1108) coupled to a mass spectrometer continuous flow isotope ratio (Thermo Scientific Delta V Advantage) through a ConFlo IV interface. The $\delta^{13}\text{C}$ values were normalized in L-SVEC-NBS-19 scale, according Coplen et al. (2006).

C3 and C4 proportions of each sample were estimated according to Carvajal et al. (2013) as follows:

$$\text{C}_{\text{C3}} = ((\delta^{13}\text{C}_{\text{SC3}} - \delta^{13}\text{C}_{\text{SC4}}) / (\delta^{13}\text{C}_{\text{VC3}} - \delta^{13}\text{C}_{\text{SC4}})) \times \text{C} [\%]$$

$$\text{C}_{\text{C4}} = ((\delta^{13}\text{C}_{\text{SC4}} - \delta^{13}\text{C}_{\text{SC3}}) / (\delta^{13}\text{C}_{\text{VC4}} - \delta^{13}\text{C}_{\text{SC3}})) \times \text{C} [\%]$$

Where $\delta^{13}\text{C}_{\text{SC3}}$ is the natural abundance of C in soil corresponding to C3 plants; $\delta^{13}\text{C}_{\text{SC4}}$ is the natural abundance of $\delta^{13}\text{C}$ in the soil corresponding to C4 plants; $\delta^{13}\text{C}_{\text{VC3}}$ and $\delta^{13}\text{C}_{\text{VC4}}$ is the natural abundance of $\delta^{13}\text{C}$ in leaf plant tissues of C3 plants ($\delta^{13}\text{C}$ average of *Sarcocornia perennis* and *Limonium brasiliense*) and C4 plants (*Spartina alterniflora*), respectively, and C is the soil carbon content.



Legend

	Sandy beach ridges		Piedmont slope (bajada)		Tidal channels
	Tidal flat		Littoral pediment (Middle Miocene sedimentary rocks)		Sand bars
	Salt pans (bare soils)		Vegetation community dominated by <i>Spartina alterniflora</i>		Soil profiles
	Alluvial fan		Vegetation community dominated by <i>Limonium brasiliense</i>		Topographic transect
	Holocene Beach ridges		Vegetation community dominated by <i>Sarcocornia perennis</i>		Piezometers

Fig. 3. Geomorphological sketch of the Fracasso salt marsh showing the topographic transects (P1 and P2), groundwater piezometers, soil sampling profiles and its associated vegetation units.

3. Results

3.1. Landforms and landscape characteristics

According to Pye and French (1993), Fracasso salt marsh was classified as open marsh coast, since it is affected by the predominant influence of marine action, which is principally protected both by sand bars which stand parallel to the coastline and by a small modern recurved spit developed towards the west of the marsh. The restrictive effect of wave action to develop the salt marsh was produced by a series of parallel sand bars, which were formed by sediment accretion from the mainland to the sea due to the influence of waves and the littoral drift. This littoral drift was mainly manifested from SW to NE and was recorded by a small modern recurved spit towards the west of the study area (Fig. 3). However, a paleo spit (small and recurved) was observed towards the east of the salt marsh with NE-SW direction indicating another current component. Return currents at low tide were those that produced the perpendicular channels to the coast cutting the bars almost completely; then, these channels in turn were connected by inter-bars channels.

The low position of the salt marsh was colonized by *Spartina alterniflora* (Sa), where the waterlogged conditions were almost permanent due to daily tides. In this sector the upper limit of the saturated zone was near to the surface, registering anoxic conditions throughout the soil profile. The tidal channels that cross the tidal plain had a meandering habit. Erosion occurred on the concave (internal) face with formation of levees at the top. On the convex face (external) sedimentation occurred (point bars) at the lower physiographic level (colonized also by *Spartina alterniflora*). The tidal channel levees were a few meters wide which were highlighted by the dominance of *Limonium brasiliense* accompanied with *S. perennis*. The inner marsh, the tidal flat was dominated mainly by *Sarcocornia perennis*, while at the higher marsh, where it was only reached by syzygy tides (towards the continental sector), the *S. perennis* community was accompanied by *L. brasiliense* and a few isolated *S. densiflora* plants. In these sectors, the drainage network in this landform that resulted from the flat slope and the preexisting microtopography, showed a dendritic or meandriform-dendritic pattern.

Table 1
Physical and chemical properties of Fracasso salt marsh soils.

Pedons	Depth	Colour (moist)	Structure ^a	Boundary ^a	Sand	Silt	Clay	pH	Eh	pHi	pHinc	pHp	CaCO ₃	C	N	C:N	δ13C
Horizons	(cm)	matrix – mottles				(%)		field	(mV)				(%)				(‰)
<i>(Sa1) Sodic Endoaquent</i>																	
Ag1	0–8	5Y 5/2–7.5 YR 3/3	sg	sw	19.6	74.6	5.8	6.8	–45.0	6.9	6.6	2.2	0.1	5.9	0.37	15.8	–18.3
Ag2	8–17	5Y 5/2–7.5 YR 3/3	sg	aw	27.8	68.4	3.9	6.9	–314.8	7.6	5.7	2.1	0.2	3.4	0.14	24.9	–17.9
2Cg	> 17	5Y 6/6	sg	–	78.2	19.3	2.5	7.1	–308.2	7.8	8.0	2.0	0.4	1.0	0.06	16.1	–20.3
<i>(Lb1) Typic Fluvaquent</i>																	
A	0–7	10 YR 5/3	sg	aw	44.0	54.1	1.9	7.4	101.2	7.3	7.8	4.6	1.2	3.3	0.18	17.8	–21.2
C	7–40	10 YR 6/3	sg	as	94.2	4.3	1.5	7.3	137.0	7.2	7.2	3.2	0.6	0.3	0.01	40.5	–22.3
2Cg1	40–73	10 YR 6/1 – 5 YR 5/4	sg	aw	15.8	72.4	11.8	6.4	193.6	6.6	6.5	3.4	0.2	2.8	0.14	20.4	–19.9
3Cg2	> 73	5Y 6/2	sg	–	92.9	5.6	1.5	6.2	213.2	6.6	6.8	3.9	0.7	0.2	0.01	32.8	–19.5
<i>(Sp1) Typic Fluvaquent</i>																	
Ag1	0–18	7.5 YR 5/2	sg	gw	5.9	91.3	2.8	6.8	121.2	7.6	7.9	5.9	1.7	3.3	0.14	23.4	–24.0
Ag2	18–32	7.5 YR 5/2	sg	aw	7.9	89.2	2.8	6.8	147.2	7.3	7.6	6.8	0.6	2.5	0.11	22.3	–22.0
Cg1	32–58	10 YR 6/2 – 5 YR 4/6	sg	aw	10.2	86.0	3.8	6.9	174.6	7.0	6.9	4.3	0.3	3.2	0.15	21.0	–20.8
2Cg2	> 58	7.5 YR 3/0	sg	–	51.7	47.5	0.9	7.4	149.6	7.0	7.2	4.5	0.3	1.1	0.05	19.7	–20.1
<i>(Sa2) Sodic Psammaquent</i>																	
Ag	0–32	10 YR 4/1	sg	gs	96.8	2.8	0.5	6.9	–260.4	7.5	6.6	3.4	0.2	0.3	0.04	6.2	–19.5
Cg	> 32	10 YR 4/0	sg	–	96.2	3.3	0.5	7.1	–313.8	7.7	6.0	2.8	0.2	0.2	0.01	13.4	–21.6
<i>(Lb2) Typic Fluvaquent</i>																	
A1	0–10	10 YR 5/3	sg	aw	14.6	78.6	6.8	7.5	155.7	7.2	7.5	4.1	0.4	4.2	0.23	18.2	–21.4
2A2	10–35	10 YR 6/3	sg	as	18.4	68.8	12.8	6.9	226.5	7.2	7.1	3.8	0.4	2.2	0.10	23.1	–21.3
3C	35–75	10 YR 5/2	sg	as	90.4	8.1	1.5	7.1	221.5	7.0	7.2	3.7	1.0	0.3	0.02	12.9	–21.5
3Cg	> 75	7.5 YR 3/0	sg	–	92.9	5.7	1.5	6.3	56.5	7.0	4.2	1.3	0.3	0.2	0.01	26.0	–17.9
<i>(Sp2) Typic Fluvaquent</i>																	
Ag1	0–12	7.5 YR 5/2	gr	as	11.0	87.1	1.8	7.7	146.2	7.7	8.1	7.2	1.4	2.6	0.11	23.7	–21.2
Ag2	12–27	7.5 YR 5/2	sg	gs	41.6	57.6	0.9	7.2	205.4	7.0	7.3	7.0	0.4	1.5	0.07	19.6	–20.2
2Cg1	27–75	10 YR 6/2 – 5 YR 4/6	sg	gs	75.6	22.5	1.9	6.7	175.2	6.8	7.1	3.8	0.2	0.4	0.04	11.1	–18.2
2Cg2	> 75	7.5 YR 3/0	sg	–	88.2	10.3	1.5	6.7	–101.8	7.1	3.7	1.9	0.1	0.4	0.03	16.7	–18.5

^a Abbreviations for morphological description are from Schoeneberger et al. (2012); structure: gr granular, sg single grain, m massive, pl platy, pr prismatic, sbk subangular; boundary, distinctness: a abrupt, g gradual; topography: w wavy, s smooth, i irregular.

3.2. Soil-geomorphic relationship

The morphological soil descriptions (Table 1) show sedimentological discontinuities, which delimit successive depositional units, occurred during marsh landscape evolution. The *n*-values were < 0.7 in all soil horizons. The Sa soils occurred in sand bars environments; Sa1 soil developed in the inter-bar area, where clay and silt particles were deposited, evolving to the sequence Ag1-Ag2 horizons. This horizon sequence overlaid the 2Cg horizon with sandy texture corresponding to the foot-slope of the sand bar. The main redoximorphic feature found in this soil was constituted by a depleted matrix in the Ag horizons (value ≥ 4 and chroma ≤ 2, Munsell soil color chart; Schoeneberger et al., 2012), with few pore linings (root channels) in the upper part of the Ag1 horizon (Fig. 4a). On the other hand, Sa2 soil developed at the top of a sandy bar and the soil horizon sequence was Ag-Cg. (Fig. 4b). The redoximorphic features were represented by a reduced matrix (value ≥ 4 and chroma ≤ 2, Munsell soil color chart), which smells of rotten eggs, indicating the occurrence of sulfides, and therefore, strongly reduced conditions (Mitsch and Gosselink, 1993, Fig. 4b). Lb soils developed on the highest topographic position of the salt marsh. The horizon sequence of Lb1 profile was: A-C-2Cg1-3Cg2. It was also flooded by periods of extraordinary tides (according to the maximum height of syzygy tides, National Hydrography Service) and sporadically received sandy material by overflowing the adjacent tidal channels (levee deposit, C horizon). The water table at the moment of the profile

description was 87 cm deep. The redoximorphic features were principally composed of redox concentrations (hue 5 YR) in stratified sediments (soil discontinuities; Fig. 4c). Just as the Lb1 soil, the Lb2 soil was developed on levee deposits, but the *L. brasiliense* community was associated with *S. perennis* in a proportion of 60:40. The profile sequence was A1-2A2-3C-3Cg and the water table at the moment of the profile description was 75 cm deep. Unlike soil Lb1, the superficial A1-2A2 horizons (levees deposits) had a silt loam texture. The redoximorphic features were composed of pore linings such as aerenchymes and roots imprints (rizho-concretions) in superficial horizons while in the deepest horizons (3C-3Cg), diffuse reddish-brown nodules were observed in water-table fluctuation zone (Fig. 4d).

The Sp soils are flooded during extraordinary tides and are subject to great dry (desiccation) periods (according to the tide table values of National Hydrography Service). The water tables at the time of sampling were from 63 to 76 cm deep. The Sp1 soil presented a sequence of horizons Ag1-Ag2-Cg1-2Cg2. The Ag1-Ag2-Cg1 horizon sequence had a predominant silt texture, while the horizon 2Cg2 was mostly composed of sandy loam, indicating a discontinuity due to abrupt textural change caused by changes in sedimentation. The Cg1 horizon presented abundant redoximorphic features composed of redox concentration as pore linings (roots imprints) and diffuse nodules (Table 1; Fig. 4e). The Sp2 had the soil sequence Ag1-Ag2-2Cg1-2Cg2 and the same soil morphology as Sp1 soils, evidenced also by the homogeneous vegetable cover of this landscape unit (Fig. 4f).

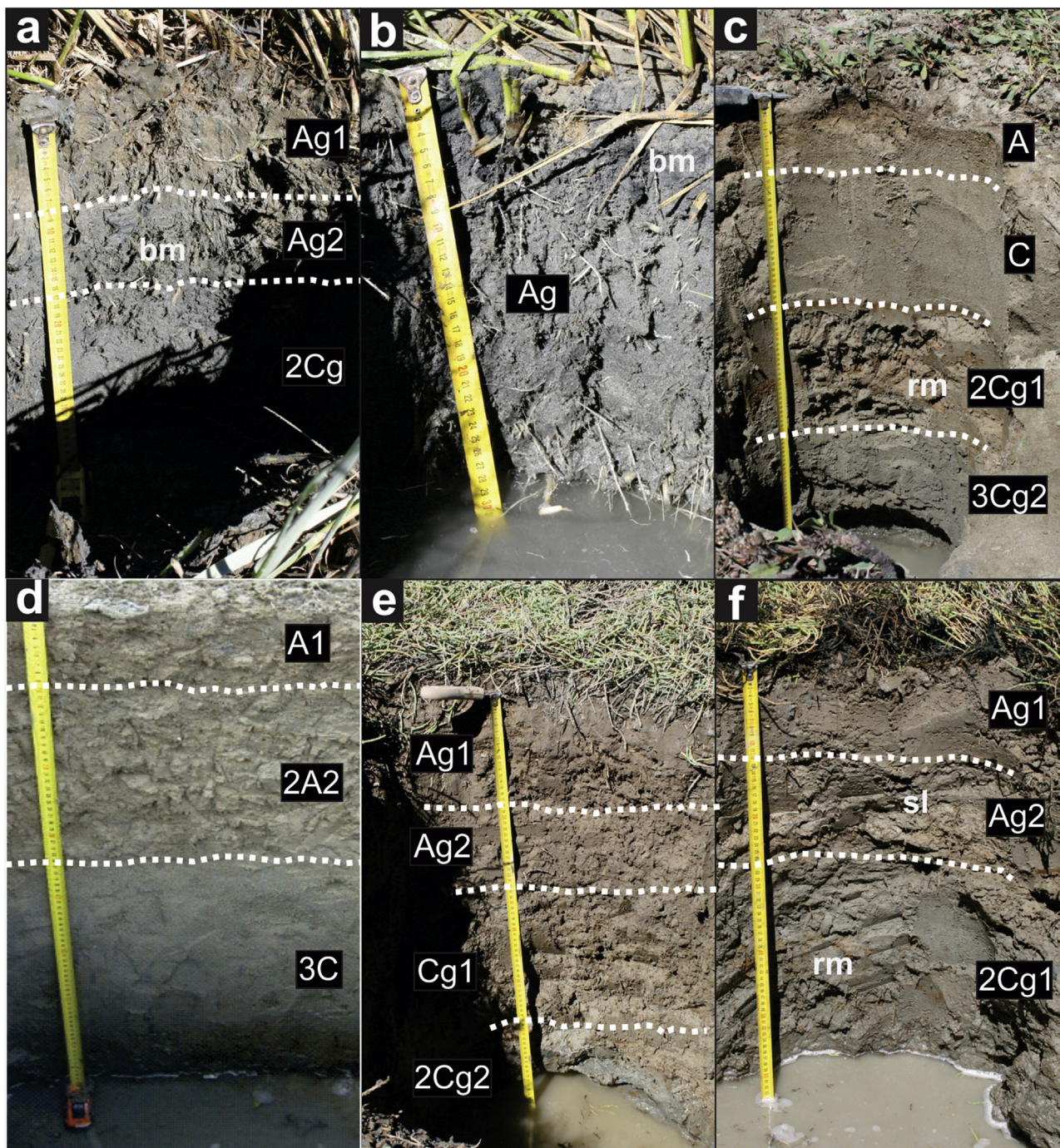


Fig. 4. Fracasso soils profiles and classification. **a** Sodic endoaquent (Sa1,**a**) and Sodic Psammaquent (Sa2,**b**) in *Spartina alterniflora* and Typic fluvaquent in *Limonium brasiliense* (Lb1,**c**; Lb2,**d**) and *Sarcocornia perennis* (Sp1,**e**; Sp2,**f**). *bm* black mottled; *rm* red mottled; *gm* grey mottled, *sl* sand lens. (For interpretation of the references to color in this figure legend, the reader is referred to the Web version of this article.)

3.3. Analytical determinations

The pH field increased with depth in Sa1 and Sa2 soils while it decreased with depth in Lb1, Lb2 and Sp2 soils. On the other hand, the Eh values decreased with depth, except in Lb1 soil, where a slight increase in potential redox with depth was observed in the sandy 3Cg2 horizon (Table 1). In Sp1 soil potential redox remained practically constant with depth. The decrease incubation pH values (Table 1) was not enough to diagnose sulfidic materials; only the deep horizons of Sp2 and Lb2 soil reached values of pH 3.7 and 4.2, respectively. In superficial horizons of Lb and Sp soils, a slight rise of incubation pH was

recorded. The pH values fell drastically in the deepest horizons Sa1, Lb2, and Sp2 soils after hydrogen peroxide treatment, which denoted the presence of sulfidic materials (pyrite) and therefore the occurrence of potential acid sulfate soils (PASS; Ahern et al., 1998; Alsemgeest et al., 2005). The SEM-EDS analysis (Fig. 5) indicated the presence of sulfidic material registered by framboidal pyrite (from French word: framboise, raspberry-patterns) composed of spheroidal aggregates of octahedral pyrite microcrystals, which reached from 0.2 to 0.5 μm long. There were also isolated octahedral pyrite microcrystals. The EDS analysis showed the S-Fe relation (2:1) indicating the pyrite formula.

The carbonate contents reached the maximum value (1.7%) in Ag1

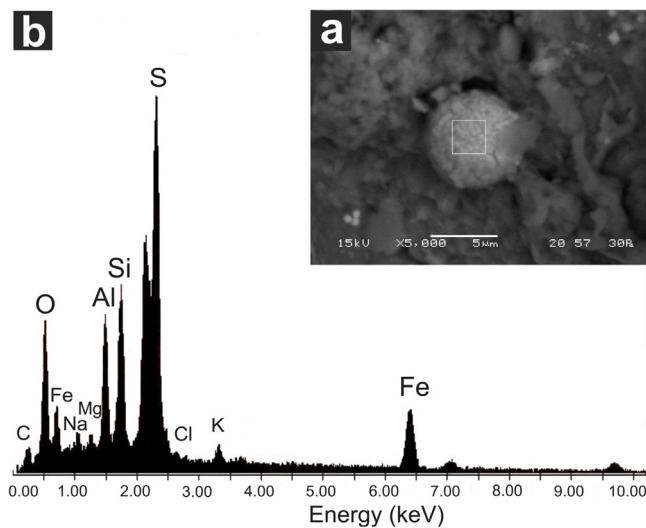


Fig. 5. a SEM Mycrophotography of a pyrite framboid composed of octahedral microcrystals (center) and a few isolated microcrystals (bottom left and top right) and, b EDS spectrum showing sulphur and ferrum dominance (2:1); both obtained from the *Sarcocornia perennis* deepest soil horizon (2Cg2, Sp2) in Fracasso salt marsh.

horizon of Sp1 soil, probably due to shell fragments observed in the field and during soil sieving. As regards to macronutrients, total soil nitrogen values did not exceed 0.4% in the studied soils, while organic carbon reached 6% in Ag1 horizon of Sa1 soil. The C and N contents indirectly varied with sand fraction contents (Table 1).

The pH values in the 1:2.5 soil-water extract (Table 1) were neutral to moderately alkaline in the surface and subsurface soil horizons but they decreased with depth to extremely acidic (pH 4) in 2Cg2 horizon of Sp2 soil. Both sodium and chloride were the dominant ions (Table 2) followed by sulfate and magnesium because the chemistry of the water table and soil solution was influenced by the sea water. The dominance of Na^+ versus Ca^{2+} and Mg^{2+} ($\text{ESP} > 15\%$) and a high value of EC ($> 4 \text{ dS m}^{-1}$), met the conditions of saline-sodic soils (U.S. Salinity Laboratory Staff, 1954). The CEC in these soils reached maximum values of $67.3 \text{ cmol}_{(\text{c})} \text{ kg}^{-1}$ in the Ag1 horizon of Sp1 soil, while a minimum value of $2.5 \text{ cmol}_{(\text{c})} \text{ kg}^{-1}$ was recorded in the deepest C horizons of Lb1 and Sa2 soils.

Regarding the groundwater characteristics, the samples obtained from monitoring network (Fig. 3) showed soluble salt contents higher than the marine water in all piezometers, with fluctuations associated mostly with the evapotranspiration process and the inflow frequency. The sample located near the upped edge of the salt marsh was also influenced by continental groundwater flow. The groundwater pH values ranged from 6.7 to 7.3 and the Eh values were positive in most of the samples. The major ions contents indicated that the groundwater type that dominates was the Na-Cl type (Table 5).

Table 2
Chemical composition of soil solutions from Fracasso salt marsh soils extracts.

Pedons	Depth	pH	CE	Na^+	K^+	Ca^{2+}	Mg^{2+}	Cl^-	SO_4^{2-}	$\text{SO}_4^{2-}/\text{Cl}^-$	ESP	CEC
Horizons	(cm)	1:2.5	(dS/cm)	(meq/l)							(%)	(cmol/kg)
<i>(Sa1) Sodic Endoaquent</i>												
Ag1	0–8	6.3	36.7	515.2	7.4	19.3	155.1	594.6	20.7	0.03	44.5	41.8
Ag2	8–17	4.1	27.8	387.7	6.0	13.7	89.6	392.8	23.8	0.06	43.9	29.9
2Cg	> 17	5.3	12.2	126.4	4.7	10.1	33.2	131.7	10.5	0.08	27.9	10.3
<i>(Lb1) Typic Fluvaquent</i>												
A	0–7	7.8	13.9	139.4	4.5	3.4	25.9	160.0	4.6	0.29	34.4	26.0
C	07–40	7.2	4.3	41.7	1.3	1.2	11.9	41.9	0.0	0.00	18.6	2.5
2Cg1	40–73	6.6	23.7	304.5	6.5	10.7	58.0	352.4	12.1	0.03	43.0	46.1
3Cg2	> 73	6.8	9.5	104.5	1.9	3.2	18.3	112.4	2.7	0.24	31.4	3.7
<i>(Sp1) Typic Fluvaquent</i>												
Ag1	0–18	8.2	14.7	183.7	4.7	6.1	19.7	184.9	5.7	0.03	42.6	67.3
Ag2	18–32	7.8	17.1	206.2	4.8	6.3	23.0	209.7	6.3	0.03	43.9	48.5
Cg1	32–58	7.1	22.0	381.7	7.5	13.6	51.8	420.1	12.5	0.03	49.3	47.3
2Cg2	> 58	7.4	14.7	184.0	3.7	6.8	33.1	202.5	7.2	0.06	37.3	19.1
<i>(Sa2) Sodic Psammaquent</i>												
Ag	0–32	6.4	6.0	61.2	2.3	4.6	14.0	69.2	4.5	0.06	22.1	3.0
Cg	> 32	5.5	4.8	50.4	1.9	3.6	11.1	42.3	3.5	0.08	20.7	2.5
<i>(Lb2) Typic Fluvaquent</i>												
A1	0–10	7.7	10.6	126.8	3.3	4.5	17.3	124.7	3.4	0.03	35.7	45.3
2A2	10–35	7.2	14.7	182.4	4.0	3.6	32.8	200.7	7.8	0.04	38.2	39.2
3C	35–75	7.1	6.5	62.3	1.6	2.0	12.6	69.0	1.7	0.02	24.7	4.9
3Cg	> 75	4.2	6.6	62.5	2.2	6.6	18.0	66.9	5.2	0.08	20.0	3.1
<i>(Sp2) Typic Fluvaquent</i>												
Ag1	0–12	8.2	13.9	164.1	4.7	5.2	17.9	166.1	5.0	0.03	41.2	47.6
Ag2	12–27	8.0	13.1	162.2	3.9	4.6	23.6	178.7	5.2	0.03	38.5	29.2
2Cg1	27–75	7.3	10.2	132.3	2.6	2.7	19.4	120.7	2.8	0.02	36.5	7.0
2Cg2	> 75	4.0	9.1	96.7	2.9	7.4	20.7	113.9	8.0	0.07	26.9	6.1

Table 3
Folk and Ward parameters of Fracasso salt marsh sandy soil horizons.

	Soil/horizon	Sa1/2Cg	Lb1/C	Lb1/3Cg2	Sp1/2Cg2	Sa2/Ag	Sa2/Cg	Lb2/3C	Lb2/3Cg	Sp2/2Cg1	Sp2/2Cg2
Folk and Ward method (ϕ)	Mean	2.70	2.75	2.82	2.92	2.69	2.69	2.85	2.73	2.91	2.89
	Sorting	0.51	0.32	0.30	0.41	0.40	0.36	0.40	0.33	0.47	0.41
	Skewness	-0.35	-0.71	0.15	-0.69	-1.20	-1.67	-0.61	-0.35	0.03	0.19
	Kurtosis	4.39	6.74	7.87	11.86	7.10	10.22	7.78	5.64	5.43	5.40
Folk and Ward method (Description)	Mean	f S	f S	f S	f S	f S	f S	f S	f S	f S	f S
	Sorting	mw S	vw S	vw S	w S	w S	w S	w S	vw S	w S	w S
	Skewness	Sym	c Sk	Sym	c Sk	c Sk	vc Sk	c Sk	Sym	Sym	Sym
	Kurtosis	L	L	v L	v L	L	v L	v L	L	L	L

^a Abbreviations for Folk and Ward (1957) parameters: f S fine sand, w S well sorted, vw S very well sorted, mw S moderately well sorted, c Sk coarse skewed, vc Sk very coarse skewed, Sym symmetrical, L leptokurtic, v L very leptokurtic.

Table 4
Comparative particle size distribution index of the sand fractions, between C horizons of the studied soil profiles.

Soil/horizon	Sa1/2Cg	Lb1/C	Lb1/3Cg2	Sp1/2Cg2	Sa2/Ag	Sa2/Cg	Lb2/3C	Lb2/3Cg	Sp2/2Cg1	Sp2/2Cg2
Sa1/2Cg	100									
Lb1/C	95	100								
Lb1/3Cg2	81	91	100							
Sp1/2Cg2	76	82	91	100						
Sa2/Ag	87	95	86	78	100					
Sa2/Cg	84	96	87	78	96	100				
Lb2/3C	83	88	92	89	84	84	100			
Lb2/3Cg	83	96	88	79	95	96	85	100		
Sp2/2Cg1	85	84	86	78	85	83	90	85	100	
Sp2/2Cg2	84	88	89	89	85	86	95	86	95	100

Table 5
Groundwater ionic composition of Fracasso salt marsh piezometers.

Piezometer	pH	Na ⁺	K ⁺	Ca ²⁺	Mg ²⁺	Cl ⁻	HCO ₃ ⁻	SO ₄ ²⁻	SO ₄ ²⁻ /Cl ⁻
		(meq/l)							
Lb2	7.0 ± 0.2	501.5 ± 45.2	11.7 ± 1.4	23.5 ± 1.4	116.3 ± 9.3	589.7 ± 39.5	3.0 ± 0.4	62.2 ± 5.4	0.1 ± 0.0
Sp1	6.7 ± 0.1	926.5 ± 83.0	17.9 ± 4.1	46.5 ± 4.1	206.0 ± 17.9	956.2 ± 74.7	6.3 ± 1.3	111.4 ± 11.6	0.1 ± 0.0
Sp2	7.3 ± 0.3	663.7 ± 72.9	13.9 ± 5.7	28.2 ± 5.7	124.5 ± 28.8	783.4 ± 76.5	4.0 ± 1.8	66.6 ± 9.5	0.1 ± 0.0
sea water	8.2	493.0	10.72	22.9	114.4	542.3	1.9	59.7	0.1

3.4. Grain-size distribution analysis of buried sandy soil horizons

The mean grain-size ranges (in phi values) varied from 2.915 to 2.689 phi (sand fine), and the standard deviation values ranged from 0.508 to 0.298 phi (Table 3). This sorting grade corresponds to the range of well sorted to very well sorted, except for the 2Cg horizon of Sa1 soils with sands moderately well selected (inter-bar area). The sand fractions showed very coarse skewed (0.194) to symmetrical (-1.674) distribution. Kurtosis values ranged between 4.386 (leptokurtic) to 11.859 (very leptokurtic).

The CPSDI ranged from high similarity to extremely high similarity of the sand size distribution between the horizons of each soil profile. In addition, the indexes were also generally high and extremely high between horizons of different soil profiles (Table 4); except in some pair combination of horizons from Sa and Sp soils, ranging mostly between 76 and 84. This similarity grade was also observed through cumulative frequency diagrams of the grain size distribution (Fig. 6).

3.5. Stable carbon isotope analysis of soil organic matter

The isotope composition of leaf plant tissues of *S. alterniflora*, *L. brasilense* and *S. perennis* were 14.4‰, 28.8‰ and 25.6‰, respectively. In general, the $\delta^{13}\text{C}$ of soil organic carbon (Table 1) varied between -17.9‰ and -24.0‰. In Lb and Sp soils, the isotope compositions became richer as depth increase while in Sa soils this tendency did not occur.

Even though isotopic impoverishment was observed in Sa1 as the depth increased, C4 dominated most of the Sa1 profile (Fig. 7a). But in Lb1, an inversion of the values of $\delta^{13}\text{C}$ was observed in the first two horizons, corresponding to an increase in C3 plants and a decrease $\delta^{13}\text{C}$ as the depth increased (Fig. 7b). In the case of Sp1 an isotopic enrichment was observed with the increase in depth, increasing the proportion of C4 (Fig. 7c). The same isotopic fluctuation was observed in the described soils corresponding to the P2 topographic transect (Table 1). In the case of Sa2 soil, an isotopic enrichment was observed in most of the profile and a slight isotopic impoverishment in depth with a clear dominance of C4 plants in most of the profile (Fig. 7d). Lb2 soil presented similar $\delta^{13}\text{C}$ values throughout the profile where the C3 plants dominated with the increase in depth showing an abrupt drop in the last horizon dominated by C4 (Fig. 7e). Finally, Sp2 soil presented a marked isotopic enrichment with increasing depth where the C4 was dominant in the deepest two horizons (Fig. 7f).

4. Discussion

4.1. Salt marsh geomorphology, soil development and classification

The results obtained in soil analysis showed a strong interrelationship among edaphic variables, mainly between texture and EC. For instance, the great permeability of sandy soils did not retain the salts in the soil solution and were washed by subsurface drainage. On the other hand, silts and clays had a larger specific surface area, which allowed

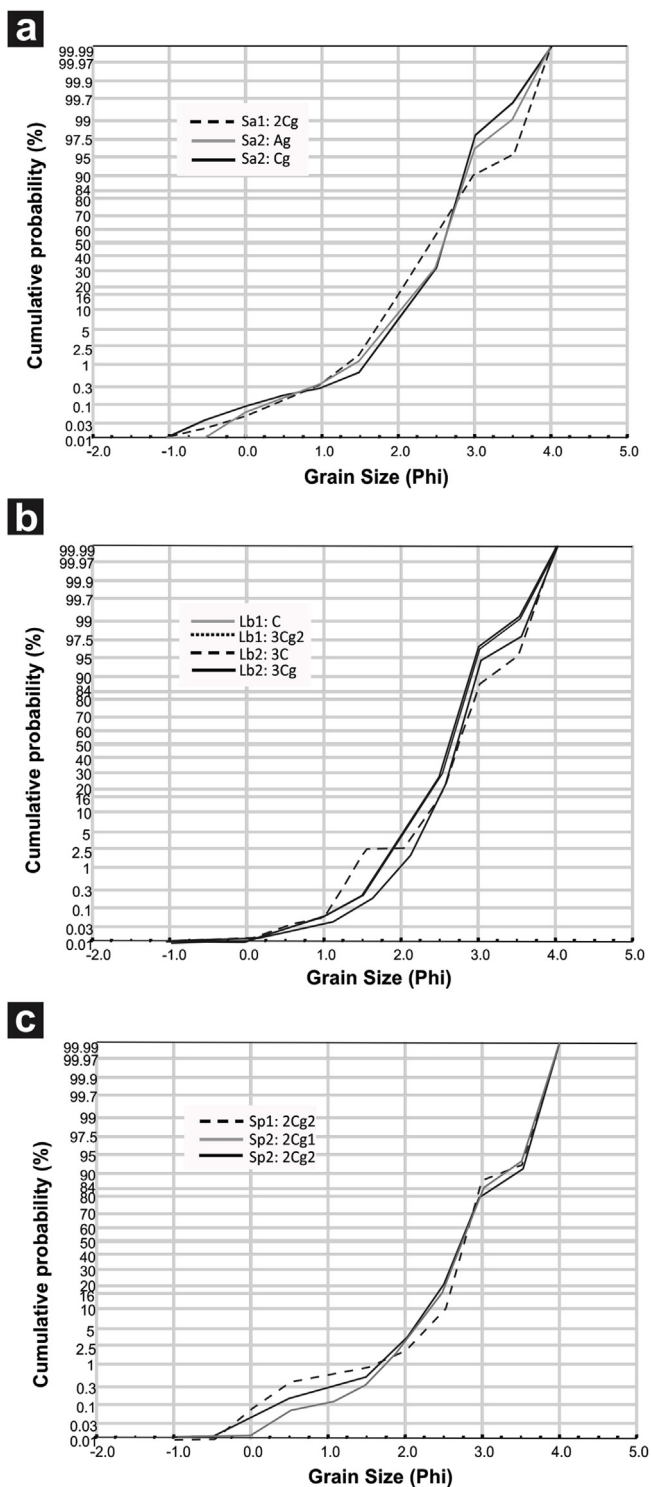


Fig. 6. Log probability plots of sandy soil horizons samples of Fracasso salt marsh soils. a *Spartina alterniflora*, b *Limonium brasiliense* and c *Sarcocornia perennis*.

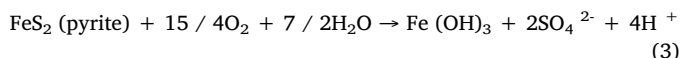
greater cohesion between the particles, favoring the retention of the soil solution and the adsorption of electrolytes on the surface of the colloids (Porta et al., 1999). This relationship can be expressed by the following equation: $EC = 21.8358 - 0.1549 \text{ sand}$, $R^2 = 0.485$ and $p = 0.005$, calculated from values of EC and sand percentage of the studied horizons (Tables 1 and 2). In this case, the sand fraction was utilized because this fraction was estimated with greater precision by gravimetry after

applying the hydrometer method. The EC increase is due to the high concentration of evaporites caused by evapotranspiration which occurs in the surface horizons of the Sp soils, where it is common to observe patches of bare soil that gradually evolve into salt-pans. According to Alvarez et al. (2016), these salt pans are built in high-level marshes and are constituted mainly by halite and gypsum/anhydrite, along with epsomite and bischofite, and the process of precipitation/dissolution of these saline crusts is the main determinant of groundwater chemistry.

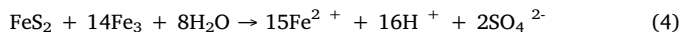
All soils are saline-sodic and have both aquic conditions and n -values < 0.7 ; although they differ in soil classification, which depends on their texture, and on both their content and their variation of organic carbon in depth. Due to these characteristics, Sa1 soil is classified as Sodic Endoaquent, while Sa2 soil (sand bar crest) is classified as Sodic Psammaquent. On the other hand, Lb and Sp soils which also show an irregular decrease in content of organic carbon are classified as Typic Fluvaquent.

Although the soils studied did not identify sulfidic materials after incubation test, these were evidenced mainly in Sa soils and in the deepest horizons from Lb1 and Sp2 soils after hydrogen peroxide treatment, classifying as potential acid sulfate soils (PASS, Ahern et al., 1998; Alsemgeest et al., 2005).

The following equation shows the acidification process that occurs during the peroxide test:



And if the $pH < 3$ implies that there is Fe^{3+} in the soil solution, the oxidation processes occurs without presence of O_2 [Eq. (4)].



The slight rise in pH after the incubation test registered in surficial horizons of Sp and Lb soils could indicate a destruction of organic acids by oxidation (Alsemgeest et al., 2005). The inhibition of pyrite oxidation during aerobic incubation could be due to buffering properties, as carbonates contents (shell fragments) and high soil cation exchange capacity provided by clay minerals and/or by organic matter (Table 1). The rapid-acidification process generated by hydrogen peroxide treatment could be producing a breakdown of the buffering mechanism when a quick oxidation is produced (Van Breemen, 1975). In addition, this delay in the pyrite oxidation rate may be influenced by the formation of oxy-hydroxide of Fe and Al and silica coatings (Zhang and Evangelou, 1996, 1998; Otero and Macías, 2001).

In general, the pH-Eh relationship measured at the field (Table 1) is commonly associated with anoxia intensity in depth (Patrick and Delaune, 1972). However, the slight increase in redox potential in the 3Cg2 horizon of Lb1 soil can be related to oxygenate and nutrient-rich seawater that easily flows across the sandy deposits that underlie silt loam 2Cg1 horizon. This redox potential pattern was observed in the deepest gravelly deposits (buried Holocene beach ridges) of other marine environments along the Patagonian coast (Esteves and Varela, 1991; Bouza et al., 2008, 2017).

The decrease in depth of pH 1:2.5 soil-water extract could be due to acid sulfuric generation by oxidation of sulfides during air drying. This process was determined by the SO_4^{2-}/Cl^- ratio, which is 0.105 in seawater (Giblin, 1988; Hounslow, 1995; Araújo et al., 2012). Also, this ratio was similar to groundwater sampled in piezometers located next to Sp1, Sp2, Lb1 and Lb2 soil profiles (Table 2), and from seawater in the study site, with values around 0.1 (Alvarez et al., 2015); lower values of SO_4^{2-}/Cl^- ratio suggest the occurrence of sulfate reduction and the synthesis of metal sulphides, whereas a higher value suggests their oxidation. The SO_4^{2-}/Cl^- ratio is higher than in seawater in the Sa1 and Sa2 soils and deepest soil horizons of Lb2 and Sp2 soils. These soil horizons also have Eh values < 0 and sulfidic materials identified by peroxide treatment.

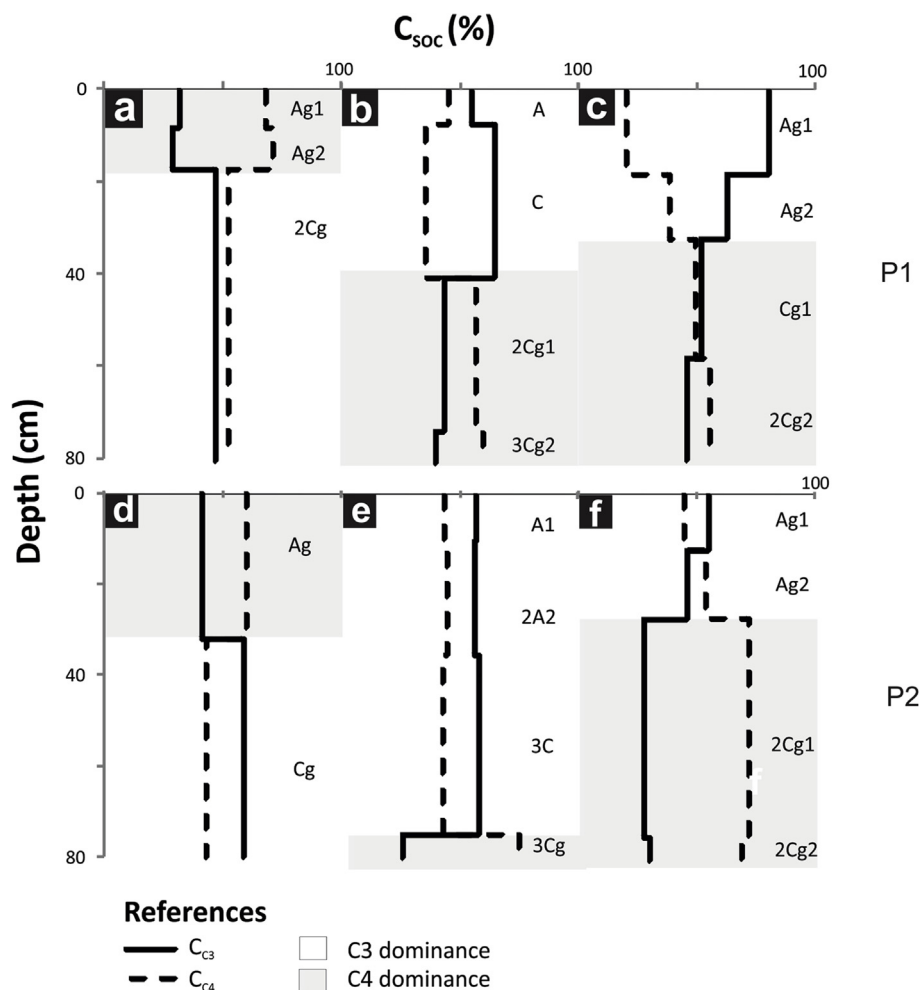


Fig. 7. Plant photosynthesis pathway (C3 and C4) distribution in depth throughout the soil topographic transects (P1 and P2). *S. alterniflora* soil profiles (Sa1, Sa2, a and d); *L. brasiliense* soil profiles (Lb1, Lb2, b and e); *S. perennis* soil profiles (Sp1, Sp2, c and f).

4.2. Sedimentation units and isotopic values relationship

The CPSDI and the cumulative frequency diagrams of the grain size distribution indicate the relative high similarity grade between horizons from actual sand bars (Sa soils) and the soil parent materials of sandy C horizons developed on the high-level salt marsh (Lb and Sp soils), thus showing a common sedimentary deposition environment. Also the mean grain-size of all samples analyzed is sand fine, indicating a high homogeneity grade and a beach sedimentary environment (Mazzoni, 1978). This beach environment is characterized by the standard deviation, which measures the sorting of sediments and indicates the fluctuations in kinetic energy or velocity conditions of depositing agent (Sahu, 1964). Thus, the range between moderately well sorted to very well sorted (values < 0.50 phi) of the studied samples, suggests the continuous action of the waves by the ebb and flow action, and a negative to slightly positive skewed sediment would indicate a beach sedimentary environment (Friedman, 1961; Andrews and van der Lingen 1969).

The organic carbon preserved in soil horizons is mainly of terrestrial origin (C:N > 12), and thus could be associated with vascular vegetation developed in the salt marsh. On the other hand, the $\delta^{13}\text{C}$ composition of the soil organic matter, both in surficial and buried sandy horizons (old beach levels) could be an indicator of vegetation shift, succession processes and salt marsh evolution (e.g. sea-level indicators).

As expected, the C4 provenance in soil organic matter of surficial horizons in low marsh level soils derived from actual *Spartina alterniflora* (Sa soils), while the C3 provenance derived from actual *Limonium brasiliense* and *Sarcocornia perennis* at low and high levels. However, the

isotopic signature in soil organic matter of subsurficial and deepest C horizons indicates a dominance of C4 plant; so if this soil parent material corresponds to old beach levels, the original installed vegetation could be *Spartina* species (Ainouche et al., 2004) constituting a pioneer marsh. The presence of salt marsh plant with C4 photosynthetic metabolism such as *S. densiflora*, could be interfering with these determinations since the isotopic values corresponding to gender *Spartina* are practically the same for both species found in these marshes but in different topographic levels which is present in topographically high isolated areas in Fracasso. Nevertheless, the sedimentological component of the deepest sandy C horizons indicates a low tide area or beach levels that would belong to *Spartina* species. In this case, the grain-size analysis was useful to determine the sedimentary environment, as skewness is environment dependent (Friedman, 1961).

The C4 plant dominance was detected in the deepest high salt marsh soil profiles from 40 to 75 cm deep and considering that the total accretion rate in Fracasso salt marsh was estimated in 0.24 cm/year (Ríos, 2015), it could be inferred that a C4 plant was present since 200–300 years old which is consistent with the *S. alterniflora* colonization hypothesis proposed by Bortolus et al. (2015). According to these authors there are no records of the *S. alterniflora* presence on the South American Atlantic coast until approximately two to three centuries ago. These studies are mainly based on a review of herbarium collections, on historical floristic descriptions and on extensive literature that supports the controversial hypothesis that the plant was introduced accidentally on the South America Atlantic coast by the water from ballast or wood from merchant vessels.

5. Conclusion

Fracasso salt marsh soils were classified as Entisols, Suborder Aquents. Particularly, *Spartina alterniflora* soils (Psammaquents and Sodic Endoaquents) were associated to sand bars environments. These soils were also considered potential acid sulfate soils (PASS) because of the presence of sulfide materials (Pyrite). On the other hand, *Limonium brasiliense* and *Sarcocornia perennis* (both Typic Fluvaquents) were associated to tidal channel levees and intertidal plains, respectively. For all from above we conclude that at great group level, a strong relationship between soil, landform and vegetation could be established. The challenge for future studies will be integrate these relationships in ecological studies (e.g. competition) in order to understand better these complexes interactions.

As regard salt marsh landscape evolution, our results indicate the presence of old sandy intertidal plains corresponding to ancient or pioneer salt marsh which is consistent with the Holocene salt marsh development, when geomorphological and sedimentological processes took place to perform the current Fracasso salt marsh. Further studies, such as ^{14}C radiocarbon dating of soil organic matter (e.g. accelerator mass spectrometry, AMS) should be done in order to establish precisely when these processes occurred. Furthermore, C4 plant species identification (e.g. phytolites analysis) is necessary to corroborate *S. alterniflora* invasion.

Finally, this study constitutes an important contribution to the salt marsh knowledge in the protected area of Península Valdés and should be extended to other Patagonian salt marshes.

Acknowledgements

The authors wish to thank Claudia Sain and Estela Cortés for their exceptional assistance at fieldwork and laboratory. We also greatly appreciate the reviewers for their comments and suggestions. This work is based on the Doctoral Thesis defended by the first author at the Universidad Nacional de Córdoba in 2015. This research has been funded by the Consejo Nacional de Investigaciones Científicas y Tecnológicas (CONICET, Grant number: PIP 2014 00190 CO, and 191) and Agencia Nacional de Promoción Científica y Tecnológica (Grant number: PICT 2013-1876).

References

Ahern, C.R., Ahern, M.R., Powell, B., 1998. Guidelines for Sampling and Analysis of Lowland Acid Sulfate Soils (ASS) in Queensland. Department of Natural Resources, Indooroopilly, Queensland, Australia, pp. 28–30.

Ainouche, M.L., Baumel, A., Salmon, A., Yannic, G., 2004. Hybridization, polyploidy and speciation in *Spartina* (poaceae). *New Phytol.* 161, 165–172.

Allen, J.R.L., Pye, K., 1992. Saltmarshes: Morphodynamics, Conservation and Engineering Significance. Cambridge University Press.

Allen, J.R.L., Haslett, S., Rinkel, B., 2006. Holocene tidal palaeochannels, Severn Estuary Levels, UK: a search for granulometric and foraminiferal criteria. *Proc. Geologists' Assoc.* 117, 329–344.

Alsemgeest, G.P., Dale, P.E., Alsemgeest, D.H., 2005. Evaluating the risk of potential acid sulfate soils and habitat modification for mosquito control (runneling) in coastal salt marshes: comparing methods and managing the risk. *Environ. Manag.* 36, 152–161.

Alvarez, M.P., Carol, E., Bouza, P., 2016. Precipitation/dissolution of marine evaporites as determinants in groundwater chemistry in a salt marsh (Península Valdés, Argentina). *Mar. Chem.* 187, 35–42.

Alvarez, M.P., Dapeña, C., Bouza, P.J., Ríos, I., Hernández, M.A., 2015. Groundwater salinization in arid coastal wetlands: a study case from Playa Fracasso, Patagonia, Argentina. *Environmental Earth Sciences* 73, 7983–7994.

APHA, AWWA, WPCF, 1997. Standard Methods for Examination of Water and Wastewater. American Public Health Association, Washington, DC.

Amoroso, R.O., Gagliardini, D.A., 2010. Inferring complex hydrographic processes using remote-sensed images: turbulent fluxes in the Patagonian gulfs and implications for scallop metapopulation dynamics. *J. Coast Res.* 26, 320–332.

Andrews, P.B., Van der Linden, G.J., 1969. Environmentally significant sedimentologic characteristics of beach sands. *New Zealand Journal of Geology and Geophysics* 12, 119–137.

Araújo, J.M.C., Otero, X.L., Marques, A.G.B., Nóbrega, G.N., Silva, J.R.F., Ferreira, T.O., 2012. Selective geochemistry of iron in mangrove soils in a semiarid tropical climate: effects of the burrowing activity of the crabs *Ucides cordatus* and *Uca maracoani*. *Geo Mar. Lett.* 32, 289–300.

Bala, L.O., Hernández, M.A., Musmeci, L.R., 2008. Humedales Costeros Y Aves Playeras Migratorias. CENPAT, Puerto Madryn, pp. 120.

Balsillie, J.H., Donoghue, J.F., Butler, K.M., Koch, J.L., 2002. Plotting equation for Gaussian percentiles and a spreadsheet program for generating probability plots. *J. Sediment. Res.* 72, 929–933.

Benito, I., Onaindia, M., 1991. Estudio de la distribución de las plantas halófilas y su relación con los factores ambientales en la marisma de Mundaka-Urdaibai. Implicaciones en la gestión del medio natural. *Eusko Ikaskuntza. Cuadernos de la sección Ciencias Naturales*, (8). pp. 116.

Bertness, M.D., 1991. Zonation of *Spartina patens* and *Spartina alterniflora* in new England salt marsh. *Ecology* 72, 138–148.

Blott, S.J., Pye, K., 2001. GRADISTAT: a grain size distribution and statistics package for the analysis of unconsolidated sediments. Version 4.0. *Earth Surf. Process. Landforms* 26, 1237–1248.

Bodman, G.B., Mahmud, A.J., 1932. The use of the moisture equivalent in the textural classification of soils. *Soil Sci.* 33, 363–374.

Bortolus, A., Carlton, J.T., Schwindt, E., 2015. Reimagining South American coasts: unveiling the hidden invasion history of an iconic ecological engineer. *Divers. Distrib.* 21, 1267–1283.

Bortolus, A., Schwindt, E., Bouza, P.J., Idaszkin, Y.L., 2009. A characterization of Patagonian salt marshes. *Wetlands* 29, 772–780.

Boutton, T.W., 1991. Stable carbon isotopes ratios of soil organic matter and their use as indicators of vegetation and climate change. In: En Boutton, T.W., Yamasaki, S.I. (Eds.), *Mass Spectrometry of Soils*. Marcel Dekker, New York, pp. 47–82.

Bouza, P., Ríos, I., Rostagno, C.M., Sain, C.L., 2017. Soil–geomorphology relationships and pedogenic processes in Península Valdés. In: Bouza, P., Bilmes, A. (Eds.), *Late Cenozoic of Península Valdés*. Springer Earth System Sciences, Patagonia, Argentina, pp. 161–190.

Bouza, P.J., Sain, C., Bortolus, A., Ríos, I., Idaszkin, Y., Cortés, E., 2008. Geomorfología y Características morfológicas y fisicoquímicas de suelos hidromórficos de marismas patagónicas. In: XXI Argentinian Soil Science Congress. Extended abstract. Potrero de los Funes, San Luis, Argentina, pp. 450.

Bouyoucos, G.J., 1962. Hydrometer method improved for making particle size analyses of soils. *Agronomy journal* 54, 464–465.

Bower, C.A., Reitemeier, R.F., Fireman, M., 1952. Exchangeable cation analysis of saline and alkali soils. *Soil Sci.* 73, 251–262.

Carvajal, A.F., Feijoo, A., Quintero, H., Rondón, M.A., 2013. Soil organic carbon storage and dynamics after C3-C4 and C4-C3 vegetation changes in sub- Andean landscapes of Colombia. *Chil. J. Agric. Res.* 73, 391–398.

Chmura, G., Aharon, P., 1995. Stable carbon isotope signatures of sedimentary carbon in coastal wetlands as indicators of salinity regime. *J. Coast Res.* 11, 124–135.

Choi, Y., Wang, Y., Hsieh, Y.P., Robinson, L., 2001. Vegetation succession and carbon sequestration in a coastal wetland in northwest Florida: evidence from carbon isotopes. *Global Biogeochem. Cycles* 15, 311–319.

Coplen, T.B., Brand, W.A., Gehre, M., Gröning, M., Meijer, H.A., Toman, B., Verkoouteren, R.M., 2006. New guidelines for $\delta^{13}\text{C}$ measurements. *Anal. Chem.* 78, 2439–2441.

Davies, B.E., 1974. Lost on ignition as an estimate of soil organic matter. *Soil Sci.* 38, 150–151.

Esteves, J.L., Varela, D.E., 1991. Nutrient dynamic of the Valdés bay-punta cero pond system (Península Valdés, Patagonia) Argentina. *Oceanol. Acta* 14, 51–58.

Fagherazzi, S., Marani, M., Blum, L.K., 2004. The Ecogeomorphology of Tidal Marshes. *Coastal and Estuarine Studies* 59 American Geophysical Union, Washington DC, pp. 266.

Farquhar, G.D., Ehleringer, J.R., Hubick, K.T., 1989. Carbon isotope discrimination and photosynthesis. *Annu. Rev. Plant Physiol. Plant Mol. Biol.* 40, 503–537.

Faulkner, S., Patrick, W., Gambrell, R., 1989. Field techniques for measuring wetland soil parameters. *Soil Sci. Soc. Am. J.* 53, 883–890.

Folk, R.L., Ward, W.C., 1957. Brazos River bar: a study in the significance of grain size parameters. *J. Sediment. Res.* 27, 3–26.

Friedman, G.M., 1961. Distinction between dune, beach, and river sands from their textural characteristics. *J. Sediment. Res.* 31, 514–529.

Friedrichs, C.T., Perry, J.E., 2001. Tidal salt marsh morphodynamics: a synthesis. *J. Coast Res.* 27, 7–37.

Giblin, A.E., 1988. Pyrite formation in marshes during early diagenesis. *Geomicrobiol. J.* 6, 77–97.

Goman, M., Malamud-Roam, F., Ingram, B., 2008. Holocene environmental history and evolution of a tidal salt marsh in San Francisco Bay, California. *J. Coast Res.* 24, 1126–1137.

Haller, M.J., 1981. Descripción geológica de la Hoja 43 h, Puerto Madryn, provincia de Chubut. Servicio Geológico Nacional.

Haller, M.J., Monti, A.J.A., Meister, C.M., 2001. Descripción de la hoja geológica 4363-I, Península Valdés, provincia del Chubut. *Boletín* 266. Servicio Geológico Nacional, Buenos Aires.

Hounslow, A.W., 1995. Water Quality Data: Analysis and Interpretation. Lewis Publishers, Boca Raton, Florida, pp. 416.

Idaszkin, Y.L., Bortolus, A., Bouza, P.J., 2011. Ecological processes shaping Central Patagonian salt marsh landscapes. *Austral Ecol.* 36, 59–67.

Idaszkin, Y.L., Bortolus, A., 2011. Does low temperature prevent *Spartina alterniflora* from expanding toward the austral-most salt marshes? *Plant Ecol.* 212, 553–561.

Idaszkin, Y.L., Bortolus, A., Bouza, P.J., 2014. Flooding effect on the distribution of native austral cordgrass *Spartina densiflora* in patagonian salt marshes. *J. Coast Res.* 30, 59–62.

Idaszkin, Y.L., Lancelotti, J.L., Bouza, P.J., Marcovecchio, J.E., 2015. Accumulation and distribution of trace metals within soils and the austral cordgrass *Spartina densiflora* in a Patagonian salt marsh. *Mar. Pollut. Bull.* 101, 457–465.

Idaszkin, Y.L., Lancelotti, J.L., Pollicelli, M.P., Marcovecchio, J.E., Bouza, P.J., 2017.

- Comparison of phytoremediation potential capacity of *Spartina densiflora* and *Sarcocornia perennis* for metal polluted soils. *Mar. Pollut. Bull.* 118, 297–306.
- Konsten, C.J.M., Van Breemen, N., Suping, S., Aribawa, I.B., Groenenberg, J.E., 1994. Effects of flooding on pH of riceproducing, acid sulfate soils in Indonesia. *Soil Science Society of American Journal* 58, 871–883.
- Lamb, A.L., Wilson, G.P., Leng, M.J., 2006. A review of coastal palaeoclimate and relative sea-level reconstructions using $\delta^{13}\text{C}$ and C: N ratios in organic material. *Earth Sci. Rev.* 75, 29–57.
- Lamb, A.L., Vane, C.H., Wilson, G.P., Rees, J.G., Moss-Hayes, V.L., 2007. Assessing $\delta^{13}\text{C}$ and C: N ratios from organic material in archived cores as Holocene sea level and palaeoenvironmental indicators in the Humber Estuary, UK. *Mar. Geol.* 244, 109–128.
- Langohr, R., Scoppa, C.O., Van Wambeke, A., 1976. The use of a comparative particle size distribution index for the numerical classification of soil parent materials: application to mollisols of the Argentinian pampa. *Geoderma* 15, 305–312.
- Langohr, R., Van Vliet, B., 1979. Clay migration in well to moderately well drained acid brown soils of the Belgian Ardennes. Morphology and clay content determination. *Pedologie* 29, 367–385.
- Leeuw, J., Munck, W., Olf, H., Bakker, J.P., 1993. Does zonation reflect the succession of salt marsh vegetation? A comparison of an estuarine and a coastal bar island marsh in The Netherlands. *Plant Biol.* 42, 435–445.
- Mazzoni, M.M., 1978. El uso de las medidas estadísticas texturales en el estudio ambiental de arenas. *Revista del Museo de La Plata, Obra Centenario. Geología* 4, 179–223.
- Mitsch, W.J., Gosselink, J.G., 1993. *Wetlands*. Van Nostrand Reinhold, New York, pp. 722.
- Mitsch, W.J., Gosselink, J.G., 2000. *Wetlands*. John Wiley & Sons, Inc., New York, New York 920 pp.
- Mendelssohn, I.A., Morris, J.T., 2002. Eco-physiological controls on the productivity of *Spartina alterniflora* Loisel. In: Weinstein, W.P., Kreeger, D.H. (Eds.), *Concepts and Controversies in Tidal Marsh Ecology*. Kluwer academic publisher, Dordrecht, pp. 59–80.
- Otero, X.L., Macías, F., 2001. Caracterización y clasificación de los suelos de las marismas de la Ría de Ortigueira en relación con su posición fisiográfica y vegetación (Galicia-NO de la Península ibérica). *Edafología* 8, 37–62.
- Page, A.L., Miller, R.H., Keeny, D.R., 1982. Chemical and microbiological properties. In: Dinaver, N.C. (Ed.), *Methods of Soil Analysis*. American Society of Agronomy, Madison, Wisconsin.
- Patrick, W.H., Delaune, R.D., 1972. Characterization of the oxidized and reduced zones in flooded soil. *Soil Sci. Soc. Am. J.* 36, 573–576.
- Pennings, S.C., Callaway, R.M., 1992. Salt marsh plant zonation: the relative importance of competition and physical factors. *Ecology* 73, 681–690.
- Porta, J., López Acevedo, M., Roquero, C., 1999. *Edafología para la Agricultura y el Medio Ambiente*, 2nd Ed. Mundi Prensas 218 pp.
- Pye, K., French, P.W., 1993. *Erosion and Accretion Processes on British Salt marshes. Introduction: Saltmarsh Processes and Morphology*. Cambridge Environmental Research Consultants, United Kingdom 42 pp.
- Redfield, A.C., 1972. Development of a new England salt marsh. *Ecol. Monogr.* 42, 201–237.
- Ríos, I., 2015. Relaciones edafogeomorfológicas y geoecología de plantas vasculares en marismas patagónicas: propiedades morfológicas, físicas, químicas y biogeoquímicas. Ph.D. Thesis. Universidad Nacional de Córdoba, Córdoba, Argentina, pp. 170.
- Sahu, B.K., 1964. Depositional mechanism from the size analysis of clastic sediments. *J. Sediment. Petrol.* 34, 73–83.
- Schoeneberger, P.J., Wysocki, D.A., Benham, E.C., 2012. *Soil Survey Staff. Field Book for Describing and Sampling Soils, Version 3.0*. Natural Resources Conservation Service, National Soil Survey Center, Lincoln, NE.
- Silvestri, S., Defina, A., Marani, M., 2005. Tidal regime, salinity and salt marsh plant zonation. *Estuar. Coast Shelf Sci.* 62, 119–130.
- Soil Survey Staff, 1999. *Soil Taxonomy: a Basic System of Soil Classification for Making and Interpreting Soil Surveys*, second ed. Natural Resources Conservation Service, USDA, Washington DC, USA, pp. 869 *Agricultural Handbook* 436.
- Soil Survey Staff, 2014. *Keys to Soil Taxonomy*, 12 ed. USDA Natural Resources Conservation Service, Washington, DC.
- Steers, J., 1977. *Physiography; Wet Coastal Ecosystems. Ecosystems of the World 1: Wet Coastal Ecosystems*, vol. 1977. Elsevier Scientific Publishing Co., New York, pp. 31–60.
- US Salinity Laboratory Staff, 1954. *Diagnosis and Improvement of Saline and Alkali Soils*. US Department of Agriculture Handbook, Washington, DC 60.
- Van Breemen, N., 1993. Soils as biotic constructs favouring net primary productivity. *Geoderma* 57, 183–211.
- Van Breemen, N., 1975. Acidification and deacidification of coastal plain soils as a result of periodic flooding. *Soil Sci. Soc. Am. J.* 39 (6), 1153–1157.
- Visher, G.S., 1969. Grain size distributions and depositional processes. *J. Sediment. Petrol.* 39, 1074–1106.
- Zedler, J.B., Callaway, J.C., Desmond, J.S., Vivian-Smith, G., Williams, G.D., Sullivan, G., Bradshaw, B.K., 1999. Californian salt-marsh vegetation: an improved model of spatial pattern. *Ecosystems* 2, 19–35.
- Zhang, Y.L., Evangelou, V.P., 1996. Influence of iron oxide forming conditions on pyrite oxidation. *Soil Sci.* 161, 852–886.
- Zhang, Y.L., Evangelou, V.P., 1998. Formation of ferric hydroxide-silica coatings on pyrite and its oxidation behavior. *Soil Sci.* 163, 53–62.